How to Cite:
Calderón, M. E. B., Pinos, M. V. B., & Llivizaca, K. V. M. (2022). A comparison of cephalometric measurements with conventional lateral cephalic 2D and reconstructed lateral cephalic of CBCT. *International Journal of Health Sciences*, *6*(S3), 11723–11737. https://doi.org/10.53730/ijhs.v6nS3.8813

A comparison of cephalometric measurements with conventional lateral cephalic 2D and reconstructed lateral cephalic of CBCT

Manuel Estuardo Bravo Calderón
Faculty of Dentistry, University of Cuenca
*Corresponding author email: estuardo.bravo@ucuenca.edu.ec

Marco Vinicio Bernal Pinos
Faculty of Dentistry, University of Cuenca
Email: marco.bernal@ucuenca.edu.ec

Karina Viviana Morocho Llivizaca
Faculty of Dentistry, University of Cuenca
Email: viviana.morocho96@ucuenca.edu.ec

***Abstract*---**Lateral cephalic radiography is mainly used to describe the morphology and growth of the craniofacial skeleton. It is considered a valuable diagnostic aid in orthodontics to plan treatment and evaluate the results. (1)(2) Cephalometric analyses requires identifying specific reference points and calculating various angular and linear dimensions. (3) Because cephalometry has been one of the most important diagnostic tools available to orthodontists for more than seven decades, different cephalometric norms have been published by leading physicians and researchers and it is used for: diagnosis, treatment progress, post-treatment evaluation, and research. (4) According to the orthodontic literature, other reconstructions such as lateral cephalic are known from more recent 3D cone beam computed tomography images. The attempt to develop 3D analysis and diagnosis is more interesting today. (4) (15) (23) Lateral cephalic radiographs are two-dimensional (2D) images that are used to represent three-dimensional (3D) structures. (5) Due to the different disadvantages of a 2D lateral cephalic X-ray: geometric distortion and the superposition of anatomical structures, 3D imaging has overcome the hurdle of 2D imaging by allowing orthodontists to visualize craniofacial structures without overlap or distortion.(6)(7) Two-dimensional (2D) lateral cephalic radiography is associated with different difficulties, such as it does not allow accurate identification due to the overlapping of reference points; in addition, it does not allow one to reflect the difference between the right and left sides; (8) while the new imaging

Manuscript submitted: 18 Feb 2022, Manuscript revised: 27 April 2022, Accepted for publication: 9 June 2022

techniques allow us to obtain improved 3D images, they come at a higher cost and with relatively low radiation exposure. (4)(9) Therefore, the purpose of this work is to corroborate the reliability of the cephalometric analysis through the two imaging modalities: conventional 2D lateral cephalic radiography and lateral cephalic radiography reconstructed from 3D cone-beam computed tomography.

***Keywords*---**cephalometric, conventional, lateral cephalic.

Summary

Objective

The objective of this study is to assess the reliability of the cephalometric measurements between images of conventional 2D lateral cephalic and lateral cephalic reconstructed from 3D cone-beam computed tomography.

Methods

2D CSF images and CBCT-generated cephalograms were taken from 35 participants. For all cephalometric images, nine angular measurements for Steinner analysis and five angular measures for Rickttes analysis were taken. For the statistical analysis, IBM (SPSS) Statistics Software for Windows, 25th edition was used. This programme allowed us to perform the different calculations of the normality test, the homoscedasticity test, as well as the mean and standard deviation of each measure. The T-test of related samples was used to compare cephalometric measurements in the tow-imaging modalities. In addition, the Pearson and Spearman Rho correlation was used to evaluate the relationship between these imaging modalities for cephalometric analysis.

Results

Only significant differences were found between the two-angular measures in the Steinner analysis (SNA and SNB), $p > 0.05$. For the rest of all the angular measures for the two analyses, there were no statistically significant differences ($p > 0.05$). Therefore, no important differences were found between the two-imaging modalities (2D and 3D) for the vertical cephalometric analyses of Steinner and Ricketts.

Conclusions

There were no significant differences between 2D cephalograms (CSF and cephalogram generated by CBCT) except for the two-angular measures SNA and SNB (Steinner analysis). The two cephalograms were similar in cephalometric measurements.

Practical implications

These results find that the values of cephalometric measurements in 2D and 3D scans have no differences of greater relevance.

Materials and Methods

Sample

A comparative study was carried out with a sample of 49 students aged between 24 and 33 years, from the seventh cycle of the Chair of Orthodontics I matrix 2013, of the Faculty of Dentistry of the University of Cuenca, Cuenca, Ecuador. Within the inclusion criteria, patients with dental crowding, patients with and without orthodontic treatment, and patients with intact maxillary and mandibular incisors were considered, and within the exclusion criteria, patients with moderate or severe asymmetries, cleft lip, and palate were excluded. Of the 49 patients, 14 of them were excluded due to problems in the radiographic images taken during the taking of the same. In both, the important cephalometric points were not observed enough to perform the respective analyses.

Image Modalities

Two types of images were performed; a conventional 2D lateral cephalic x-ray and the second, reconstructed lateral cephalic radiography from the 3D cone beam computed tomography, which was taken by a single operator. The students met at the radiological department to take conventional lateral cephalic radiographs. They were performed with a cephalostat machine, and for the acquisition of CBCT images, they were taken utilizing a CBCT Accuitomo 170 device with the technical parameters field of view (FOV) of 170 mm x 120 mm, cutting thickness of 0.33 mm, and a cutting interval of 0.66 mm in the Faculty of Dentistry of the University of Cuenca between the months of October and December of the year 2021.

For the taking of the conventional lateral cephalic radiography, the students were placed in earmuffs, the same ones that were fixed and placed in the horizontal plane of Frankfurt parallel to the floor, the sagittal plane was perpendicular to the x-ray beam, and the occlusion was fixed at the maximum intercuspation. Remember that students could not enter with any metal objects. (18) CBCT images were obtained with the largest field of view (FOV). Then, a previous induction was made about the programs to be used to obtain data with greater veracity and accuracy from two people who are students of the chair of orthodontics of the faculty of dentistry of the University of Cuenca to perform the cephalometric strokes, and in this way, nine angular measurements of the Steinner method and five of the Ricketts method were obtained. For the 2D and 3D cephalometric analyses that were carried out in the SIDEXIS program, the objective of this study was to check the difference in angular measurements between the different imaging modalities.

Cephalometric Measurements

In this study, the different cephalometric points were recognized (Table 1). (6) linear distances were measured and/or calculated (Table 2). (6) Angular measurements were made (Table 3). (6)

Table 1
Description of cephalometric points. (6)

Reference point	Abbreviation	Definition
Nasion	N	The midpoint of the frontonasal suture.
Chair	S	The point of the center of the bony crypt occupied by the pituitary gland.
Orbital	Or	The lowest point of the orbital flange.
Porion	Po	The point at the top of the bony ear canal.
Condyle	Co	The highest point of each mandibular condyle.
Anterior nasal spine	ENA	The most anterior midpoint of the anterior nasal spine of the maxilla.
Point A	Point A	The point of maximum concavity in the midline of the alveolar process of the maxilla.
Point B	Point B	The point of maximum concavity in the midline of the alveolar process of the jaw.
Chin	Me	The lowest midpoint of the chin at the contour of the mandibular symphysis.
Posterior nasal spine	ENP	The posterior midpoint of the posterior nasal spine of the palatine bone.
Basion	Ba	The earliest point of the foramen magnum.
Pogonion	PG	The most prominent point of the bony chin.
Gnathion	Gn	The point of the bisect of the angle formed by the tangent to the most protruding points of the lower edge of the jaw and the Nasion - Pogonion line.
Gonion	Go	The point at each mandibular angle that is defined by the fall of a perpendicular from the intersection of the tangent lines to the posterior margin of the mandibular vertical branch and the lower margin of the mandibular body to the horizontal branch.
Pterygomaxillary Fossa	Pt	The upper poster point of the pterygomaxillary fossa.
Interim	I	The point located in the center of the incisal edge of the upper and lower incisors.

Xi	Xi	The point of the center of the branch of the jaw.

Table 2
Definition of cephalometric linear measurements. (6)

Linear measurements	Definition
SN	Plane that joins the center of the Turkish chair with the nasion point.
NA	Line joining nasion with point A.
NB	Line linking the nasion with point B.
SC	Line that joins chair with the condylar point.
Frankfurt Map	Line passing through the porion point and the infraorbital point.
Occlusal Plan	Line that passes through the most distal interocclusal point of contact of the first molars and through the midpoint of the overbite of the incisors.
Mandibular Plane	It is the line that joins the points gonion and gnathion.
Maxillary Plane	Distance linking the ENA with ENP.
Ba-Na	Line linking basion with nasion.
Pt-Gn	Line joining the pterygoid point with gnathion.
N- Pg	Line linking nasion and pogonion point.
Go-Me	Line linking the gonion point with chin
Xi- Pm	Line linking point Xi with suprapogonion.
Xi-ENA	Line linking Xi point with ENA
Xi- Co	A line joining point Xi to point Co.

Table 3
Definition of the angular measures to be considered for the study. (6)

Angle	Plans	Norm
Steinner angles		
SNA	SNA	82° (+ - 2°)
SNB	SNB	80° (+ - 2°)
ANB	ANB	2° (+ - 2°)
CNS	CNS	115° (+ - 2°)
SN – Md	SN – Go Gn	32°
Mx – Md	ENA ENAP – Go Gn	25°
SN – 1	SN – 1 (superior)	103°
Md – 1	Go Gn- 1(bottom)	90°
Mx – 1	ENA ENP – 1(superior)	70°
1-1	1-1	131°
Ricketts Angles		

FACIAL AXIS	Ba Na – Pt Gn	90° (+ - 3°)
FACIAL DEPTH	Po Or – N Pg	87° (+ - 3°)
MANDIBULAR PLANE	Go Me- Po Or	26° (+ - 4°)
LOWER FACIAL HEIGHT	ENA Xi – Xi Pm	47° (+ - 4°)
MANDIBULAR ARCH	Dc Xi - Xi Pm	26° (+ - 4°)

Once the different angular radiographic measurements of the Steinner and Ricketts studies were performed in the two-imaging modalities, both the conventional 2D lateral cephalic radiography and the second lateral cephalic radiography reconstructed from the 3D cone-beam computed tomography results were recorded in a database created in an Excel sheet to collect this information. Also, intraoperator and interoperator were assessed to perform cephalometries by means of intraclass correlation with coefficient tests. The reliability between evaluators was good (correlation coefficient was 0.88), and the intraoperative reliability was excellent (correlation coefficients for the two researchers were 0.94 and 0.96).

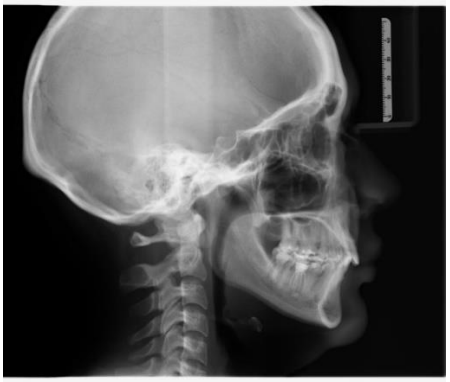

Figure 1. Conventional 2D lateral cephalic radiography. For this type of image, the different angular measurements of the Steinner and Ricketts analyses were made to verify the variability with lateral cephalic radiography reconstructed from the 3D cone beam computed tomography.

Measurements of reconstructed lateral cephalic radiography from 3D cone-beam computed tomography (CBCT) were performed in the Sidexis program. The same ones that were carried out by the two operators in which the analysis already mentioned above consisted of. (4)

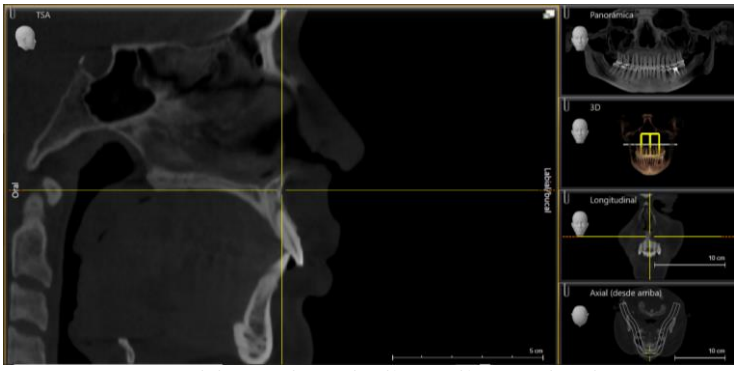

Figure 2. Reconstructed lateral cephalic radiography from 3D cone-beam computed tomography (CBCT)

For the statistical analysis, IBM (SPSS) Statistics Software for Windows, 25th edition was used to perform the different calculations of the normality test and the homoscedasticity test, and the mean and standard deviation of each measure were calculated. The T-test of related samples was used to compare cephalometric measurements in the two-imaging modalities. (11) To assess the relationship between the two-imaging modalities, Pearson and Spearman correlation coefficients were used at a level of statistical significance of 0.05.

Results

Table 4-5 summarized the statistical comparisons of the Steinner (nine-angular measures) and Ricketts (five-angular measures) measurements in the different 2D and 3D cephalometric imaging modalities. The present study identified statistically significant differences between the cephalogram 2D and 3D CBCT measurements at two-angles of the Steinner measurement (SNA p<,003; SNB p<.014). However, there are no statistically significant differences in the other angular measures of Steinner (ANB p>.160; CNS p>,522; SNGoGn p>,164; ENA-ENP GoGn p>,323; SN1 p>,530; Md1 p>,229; 1-1 p>,599). In the Ricketts Analysis, no statistically significant differences were found (Facial Axis p>,827; Facial Depth p>,561; Mandibular Plane p>,377; Lower Facial Height p>,310; Mandibular arch p>,749).

Table 4
Statistical description and comparison of cephalometric measures Ricketts 2D RCL and 3D- Cephalogram generated by CBCT

Statistical description and comparison of Ricketts cephalometric measurements of 2D RCL and 3D- Cephalogram generated by CBCT			
Variables	2D CSF Med-Desv ¶	Generated by CBCT (3D). Med-Desv ¶	P-value
Facial Axis	87,816 5,104	88,028 7,526	,857
Facial Depth	88,254 3,857	88,552 3,726	,561
Mandibular	25,129	25,720	,377

Plane	5,7551	5,423	
Lower Facial Height	45,647 5,757	46,709 5,584	,310
Mandibular Arch	33,712 6,301	33,455 7,215	,749
¶ SD: Standard deviation. ¶¶ Indicates a significant difference between the 3 imaging modalities at the confidence level of .05.			

Table 5
Statistical description and comparison of Steinner cephalometric measurements of 2D RCL and 3D-cephalogram generated by CBCT

Statistical description and comparison of Steinner cephalometric measurements of 2D RCL and 3D- Cephalogram generated by CBCT			
Variables	2D CSF Med-Desv ¶	Generated by CBCT (3D). Med-Desv ¶	P-value
SNA	83,302 4,376	85,502 5,808	,003 ¶¶
SNB	79,538 4,724	81,339 5,272	,014 ¶¶
ANB	4,117 1,862	4,194 1,839	,160
SNC	119,222 14,013	116,898 21,367	,522
SNGoGn	31,595 6,671	31,572 6,669	,164
ENA-ENPGoGn	25,378 5,946	25,528 5,942	,323
SN1	106,131 9,321	104,395 16,105	,530
Md1	95,299 6,462	95,055 7,306	,229
1-1	123,321 12,937	124,020 11,336	,599

When performing the analysis of the T-Test of related samples, data was obtained that is exposed in Table 6; in Ricketts' measurements in both 2D and 3D the following values were found:

- D-3D Facial Axis: 6,930
- 2D-3D Facial Depth: 3,011
- Mandibular Plane: 3,907
- Lower Facial Height: 6,097
- Mandibular Arch: 4,717

Similarly, the following data were discovered in the T-Test Analysis of related Steinner samples (Table 7):

- SNA 2D-3D: 3,996
- SNB 2D-3D: 4,119
- ANB 2D-3D: .581
- 2D-3D SNC: 21,263
- SNGoGn 2D-3D: .475
- ENA-ENP GoGn 2D-3D: .774
- SN1 2D-3D: 16,180
- Md1 2D-3D: 32,203
- 1-1 2D-3D: 2,593

Considering the data obtained, the standard deviation indicates that there is variability in the values collected from the statistical analysis of 2D and 3D cephalograms. In turn, the standard error helps to appreciate the values that depart from those that were obtained from the sample. (12)

Table 6
Description of data provided by T-Test of related Ricketts Analysis samples in the two 2D and 3D imaging modalities.

Testing related samples

		Related differences					t	Gl	Sig. (bilateral)
		Stocking	Deviation typ.	Desv. Average error	95% Confidence interval for difference				
					Inferior	Superior			
Par 1	2D 3D Facial Axis	-.212	6.930	1.171	-2.592	2.168	-.181	34	.857
Par 2	Prof. Facial 2D 3D	-.298	3.011	.509	-1.333	.736	-.586	34	.561
Par 3	Mandib plan. 2D 3D	-.591	3.907	.660	-1.933	.751	-.895	34	.377
Par 4	Facial Height Inf. 2D 3D	-1.062	6.097	1.030	-3.156	1.032	-1.030	34	.310
Par 5	Mandibular Arch	.257	4.717	.797	-1.363	1.878	.323	34	.749

Table 7
Description of data provided by T-Test of related samples from Steinner Analysis in the two 2D–3D imaging modalities

Testing related samples									
		Matched differences					t	Gl	Sig. (bilateral)
		Stocking	Desv. Deviation	Desv. Average error	95% confidence interval difference				
					Inferior	Superior			
Par 1	SNA (2D) - SNA (3D)	-2,200	3,996	,675	-3,572	-,827	-3,257	35	,003
Par 2	SNB (2D) - SNB (3D)	-1,801	4,119	,696	-3,216	-,386	-2,587	35	,014
Par 3	ANB (2D) - ANB (3D)	-,076	,581	,098	-,276	,122	-,782	35	,440
Par 4	SNC (2D) - SNC (3D)	2,324	21,263	3,594	-4,980	9,628	,647	35	,522
Par 5	SNGoGn (2D) - SNGoGn (3D)	,023	,475	,080	-,140	,186	,288	35	,775
Par 6	ENA ENP GoGn (2D) - ENA ENP GoGn(3D)	-,149	,774	,130	-,415	,116	-1,143	35	,261
Par 7	SN1 (2D) - SN1 (3D)	2,150	16,319	2,758	-3,455	7,756	,780	35	,441
Par 8	MD1 (2D) - MD1 (3D)	-6,670	32,203	5,443	-17,732	4,392	-1,225	35	,581
Par 9	1-1 (2D) - 1-1 (3D)	,244	2,593	,438	-,646	1,135	,557	35	,599

According to Pearson and Spearman, the correlation of the two imaging modalities in the Ricketts Analysis is significant for all angles (Facial Axis, Facial Depth, Mandibular Plane, Lower Facial Height, and Mandibular Arch) (Table 9). Similarly, in the Steinner Analysis, the correlation according to Pearson is significant for all angles, just as for Spearman, the correlation is significant for all angles (Table 8).

Table 8
Comparison of Pearson and Spearman Rho correlation coefficients in Steinner analysis in the two 2D-3D imaging modalities

Comparison of Pearson and Spearman Rho correlation coefficients in Steinner measures of 2D RCL and 3D- Cephalogram generated by CBCT		
Variables	Pearson	Spearman
SNA (2D) (3D)	,726**	,748**
SNB(2D) (3D)	,665**	,739**
ANB(2D) (3D)	,951**	,954**
SNC(2D) (3D)	,335*	,757**
SNGOGn (2D) (3D)	,997**	,995**
ENA-ENPGoGn (2D) (3D)	,992**	,981**
SN1 (2D) (3D)	,284	,738**
Md1 (2D) (3D)	,936**	,984**
1-1 (2D) (3D)	,802**	,770**
**. The correlation is significant at level 0.01 (bilateral). *. The correlation is significant at level 0.05 (bilateral).		

Table 9
Comparison of Pearson and Spearman's Rho correlation coefficients in Ricketts Analysis in the two 2D-3D imaging modalities

Comparison of Pearson and Spearman Rho correlation coefficients in Ricketts measures of the 2D RCL and 3D- Cephalogram generated by CBCT		
Variables	Pearson	Spearman
Facial Axis (2D) (3D)	.451**	.486**
Facial Depth (2D) (3D)	.685**	.719**
Mandibular Plane (2D) (3D)	.757**	.700**
Lower Facial Height (2D) (3D)	.422*	.572**
Mandibular Arch (2D) (3D)	.764**	.746*
*. The correlation is significant at level 0.05 (bilateral). **. The correlation is significant at level 0.01 (bilateral).		

Discussion

In the present study, the 2D CSF and 3D cephalograms generated by CBCT for cephalometric measurements were compared, finding a significant difference between the 2D and 3D cephalograms for two-angular measurements (SNA and SNB). In contrast, the results of Van Vlijmen et al. found that there were no statistically significant differences for several angular measures that were measured in CSF and CBCT except for two-angles, SNA and SNB. (13) (14) There were no statistically significant differences in the remaining Steinner angular measurements (ANB; CNS; SNGoGn; ENA-ENP GoGn; SN1; Md1; 1-1) and Ricketts (Facial Axis; Facial Depth; Mandibular plane; Lower Facial Height; Mandibular arch).

The anatomical structures and the different reference points were recognized and located (2D AND 3D) for the different analyses, but there is information where it is reported that NMe/SGo in the study has greater margins of error than the conventional CSF. (24) (25) In contrast, these anatomical structures and reference points could be recognized and placed in the 3D CBCT scans. (26) (27) The 3D imaging modality for orthodontic study has countless advantages over the conventional 2D imaging mode; it can be evaluated in any plane. This allows an accurate appreciation of the actual shape of the skull, jaw, and facial bones, which allows precise measurements of the relationship between them. Another of the most important advantages is the lower radiation exposure of the patient. (4). The results showed non-significant differences between the values obtained from the angular measures of the analyses. According to the normality tests applied in this study, a null hypothesis was found for all angular measurements of Ricketts and Steinner with a p> value of 0.05. (30) To determine the mean and standard deviation values of each angular measurement, both for the Steinner and Ricketts Analysis, the Homoscedasticity Test was applied, giving the following results. (Table 10 and Table 11).

Table 10
Descripción de datos proporcionados por Prueba de Homocedasticidad del Análisis de Steinner en las dos modalidades de imagen 2D-3D.

HOMOSCEDASTICITY TEST-RICKETTS ANALYSIS

	Axis Facial 2D	Axis Facial 3D	Depth Facial2 D	Depth Facial 3D	Mandibular Plane 2D	Mandibular Plane 3D	Lower Facial Height 2D	Lower Facial Height 3D	Mandibular Arch 2D	Mandibular Arch 3D
Mean	87,816	88,028	88,254	88,552	25,129	25,720	45,647	46,709	33,712	33,455
N	35	35	35	35	35	35	35	35	35	35
Desv. Typ.	5,104	7,526	3,857	3,726	5,755	5,423	5,757	5,584	6,301	7,215

Table 11
Description of data provided by the Ricketts Analysis Homoscedasticity Test in the two 2D–3D imaging modalities.

THEN	ENA ENP GoGn (2D)	ENA ENP GoGn(3D)	SN1 (2D)	SN1 (3D)	MD1 (2D)	MD1 (3D)	1-1 (2D)	1-1 (3D)
Stocking	25,378	25,528	106,131	103,981	95,299	95,055	123,321	124,020
N	35	35	35	35	35	35	35	35
Deviation	5,946	5,942	9,321	16,301	6,462	7,306	12,937	11,336
Variance		35,315	86,894	265,747	41,765	53,379	167,373	128,508

HOMOSCEDASTICITY TEST-STEINNER ANALYSIS										
	SNA (2D)	SNA (3D)	SNB (2D)	SNB (3D)	ANB (2D)	ANB (3D)	CNS (2D)	CNS (3D)	SNGoGn (2D)	SNGoGn (3D)
Stocking	83,302	85,502	79,538	81,339	4,117	4,194	119,222	116,898	31,595	31,572
N	35	35	35	35	35	35	35	35	35	35
Deviation	4,376	5,808	4,724	5,272	1,862	1,839	14,013	21,367	6,671	6,669
Variance	19,150	33,735	22,320	27,795	3,468	3,385	196,390	456,572	44,513	44,488

Subsequently, the T-test of related samples was carried out, which allows to evaluate the following aspects: mean, standard deviation, and deviation error (Table 3 and Table 4). This test is responsible for calculating the differences of each of the angular values between the two modalities (2D and 3D). This evaluation allowed to know that for Ricketts' analysis, no statistically significant differences were found in the aspects mentioned above between the two modalities. However, for Steinner's analysis, statistically, significant differences were found for the following angles: ANB, SNC, SNGoGN, ENPGoGn, SN-1, and Md-1. (28). Finally, the correlational comparison coefficient test of Pearson and Spearman was performed to analyze the different variables. This test allowed to know that if the values are 0.05, they are significant, the same as that represented with (*) and when the value is 0.01, they are significant with the

difference that is represented with (**). Within this study, all the presented values were greater than 0.05. (29)

In the present study, no statistically significant differences were found between the two 2D and 3D cephalograms (cephalograms generated by CSF and CBCT) in the cephalometric analyses used in this study, using the different tests, which is consistent with the findings of the existing research. (15) The 2D cephalogram generated by CBCT could be an alternative to the conventional 2D CSF method for those patients whose CBCT images are already available, thereby minimizing the patient's exposure to radiation and radiography costs. (16) (17) For those patients who have already obtained CBCT images, it is recommended to use their CBCT scans instead of obtaining an additional CSF to assess the vertical intermaxillary relationship. (18) (19). The validity of the different imaging modalities for evaluating vertical skeletal cephalometric measurements is still up for debate since the identification of 3D anatomical points is complex, so there is currently no standard of characteristics for proper identification. (11) (18)

Conclusions

Finally, the present study yielded values where the only significant differences between the SNA and SNB angles ($p<0.05$ value) of the Steinner analysis were determined, while the remaining angles did not present differences of greater significance. Ct scan measurements for 3D cephalometric tracing did not present clear evidence of greater efficacy and reliability compared to measurements taken in 2D shots. (21) (22)

References

1. Enoki C, Telles C de S, Matsumoto MAN. Dental-skeletal dimensions in growing individuals with variations in the lower facial height. Braz Dent J [Internet]. 2004 [citado el 21 de enero de 2022];15(1):68–74.
2. Cook AH, Sellke TA, BeGole EA. Control of the vertical dimension in Class II correction using a cervical headgear and lower utility arch in growing patients. Part I. Am J Orthod Dentofacial Orthop [Internet]. 1994 [citado el 21 de enero de 2022];106(4):376–88.
3. Kumar V, Ludlow JB, Mol A, Cevidanes L. Comparison of conventional and cone beam CT synthesized cephalograms. Dentomaxillofac Radiol [Internet]. 2007;36(5):263–9.
4. Yitschaky O, Redlich M, Abed Y, Faerman M, Casap N, Hiller N. Comparison of common hard tissue cephalometric measurements between computed tomography 3D reconstruction and conventional 2D cephalometric images. Angle Orthod [Internet]. 2011 [citado el 24 de enero de 2022];81(1):11–6.
5. Schulze D, Heiland M, Thurmann H, Adam G. Radiation exposure during midfacial imaging using 4- and 16-slice computed tomography, cone beam computed tomography systems and conventional radiography. Dentomaxillofac Radiol [Internet]. 2004;33(2):83–6.
6. Pittayapat P, Bornstein MM, Imada TSN, Coucke W, Lambrichts I, Jacobs R. Accuracy of linear measurements using three imaging modalities: two lateral cephalograms and one 3D model from CBCT data. Eur J Orthod [Internet]. 2015 [citado el 24 de enero de 2022];37(2):202–8.

7. Ramírez Huerta JV, Oropeza Sosa JG, Flores Ledesma A. Estudio comparativo entre mediciones cefalométricas en cone-beam y radiografía lateral digital. Rev mex ortod [Internet]. 2015;3(2):84–7.
8. Oh S, Kim C-Y, Hong J. A comparative study between data obtained from conventional lateral cephalometry and reconstructed three-dimensional computed tomography images. J Korean Assoc Oral Maxillofac Surg [Internet]. 2014 [cited 2022 Jan 14];40(3):123–9.
9. Afrashtehfar KI, Profesor A. Comparación entre radiografía tradicional y tridimensional en Odontología [Internet]. Medigraphic.com. [citado el 21 de enero de 2022].
10. Patel S, Harvey S. Guidelines for reporting on CBCT scans. Int Endod J [Internet]. 2021;54(4):628–33
11. Wen J, Liu S, Ye X, Xie X, Li J, Li H, et al. Comparative study of cephalometric measurements using 3 imaging modalities. J Am Dent Assoc [Internet]. 2017 [citado el 14 de enero de 2022];148(12):913–21.
12. Abraira V. Desviación estándar y error estándar. Semergen [Internet]. 2002 [citado 2022 Jan 14];28(11):621–3.
13. Afrashtehfar KI, Profesor A. Comparación entre radiografía tradicional y tridimensional en Odontología [Internet]. Medigraphic.com. [citado el 21 de enero de 2022].
14. van Vlijmen OJC, Maal T, Bergé SJ, Bronkhorst EM, Katsaros C, Kuijpers-Jagtman AM. A comparison between 2D and 3D cephalometry on CBCT scans of human skulls. Int J Oral Maxillofac Surg [Internet]. 2010 [citado el 24 de enero de 2022];39(2):156–60.
15. Jodeh DS, Kuykendall LV, Ford JM, Ruso S, Decker SJ, Rottgers SA. Adding depth to cephalometric analysis: Comparing two- and three-dimensional angular cephalometric measurements: Comparing two- and three-dimensional angular cephalometric measurements. J Craniofac Surg [Internet]. 2019 [citado el 21 de enero de 2022];30(5):1568–71.
16. Cassetta M, Altieri F, Di Giorgio R, Silvestri A. Two-dimensional and three-dimensional cephalometry using cone beam computed tomography scans. J Craniofac Surg [Internet]. 2015 [cited 2022 Jan 24];26(4):e311-5.
17. Roque-Torres GD, Meneses-López A, Bóscolo N, De Almeida SM, Neto FH. La tomografía computarizada cone beam en la ortodoncia, ortopedia facial y funcional Cone beam computed tomography use in orthodontics, functional facial orthopedics [Internet]. Org.pe. [cited 2022 Jan 21].
18. Damstra J, Fourie Z, Huddleston Slater JJR, Ren Y. Accuracy of linear measurements from cone-beam computed tomography-derived surface models of different voxel sizes. Am J Orthod Dentofacial Orthop [Internet]. 2010;137(1):16.e1-6; discussion 16-7.
19. Lagravère MO, Carey J, Toogood RW, Major PW. Three-dimensional accuracy of measurements made with software on cone-beam computed tomography images. Am J Orthod Dentofacial Orthop [Internet]. 2008;134(1):112–6.
20. Baumgaertel S, Palomo JM, Palomo L, Hans MG. Reliability and accuracy of cone-beam computed tomography dental measurements. Am J Orthod Dentofacial Orthop [Internet]. 2009;136(1):19–25; discussion 25-8.
21. Original T. Revista Mexicana de Ortodoncia [Internet]. Medigraphic.com.
22. Cattaneo PM, Bloch CB, Calmar D, Hjortshøj M, Melsen B. Comparison between conventional and cone-beam computed tomography-generated

cephalograms. Am J Orthod Dentofacial Orthop [Internet]. 2008;134(6):798–802.
23. Cook AH, Sellke TA, BeGole EA. Control of the vertical dimension in Class II correction using a cervical headgear and lower utility arch in growing patients. Part I. Am J Orthod Dentofacial Orthop [Internet]. 1994;106(4):376–88.
24. Athanasiou AE, Miethke R, Van Der Meij AJ. Random errors in localization of landmarks in postero-anterior cephalograms. Br J Orthod [Internet]. 1999 [citado el 21 de enero de 2022];26(4):273–84.
25. Ludlow JB, Laster WS, See M, Bailey LJ, Hershey HG. Accuracy of measurements of mandibular anatomy in cone beam computed tomography images. Oral Surg Oral Med Oral Pathol Oral Radiol Endod [Internet]. 2007;103(4):534–42.
26. Chien PC, Parks ET, Eraso F, Hartsfield JK, Roberts WE, Ofner S. Comparison of reliability in anatomical landmark identification using two-dimensional digital cephalometrics and three-dimensional cone beam computed tomography in vivo. Dentomaxillofac Radiol [Internet]. 2009;38(5):262–73.
27. Enoki C, Telles C de S, Matsumoto MAN. Dental-skeletal dimensions in growing individuals with variations in the lower facial height. Braz Dent J [Internet]. 2004 [citado el 21 de enero de 2022];15(1):68–74.
28. Cook AH, Sellke TA, BeGole EA. Control of the vertical dimension in Class II correction using a cervical headgear and lower utility arch in growing patients. Part I. Am J Orthod Dentofacial Orthop [Internet]. 1994 [citado el 21 de enero de 2022];106(4):376–88.
29. View of A comparative study of digital lateral radiography and virtual cone-beam computed assisted cephalogram in cephalometric measurements [Internet]. Joralres.com. [citado el 21 de enero de 2022].
30. Chan CK, Tng TH, Hägg U, Cooke MS. Effects of cephalometric landmark validity on incisor angulation. Am J Orthod Dentofacial Orthop [Internet]. 1994;106(5):487–95
31. Suryasa, W., Sudipa, I. N., Puspani, I. A. M., & Netra, I. (2019). Towards a Change of Emotion in Translation of Kṛṣṇa Text. Journal of Advanced Research in Dynamical and Control Systems, 11(2), 1221-1231.
32. Suwija, N., Suarta, M., Suparsa, N., Alit Geria, A.A.G., Suryasa, W. (2019). Balinese speech system towards speaker social behavior. Humanities & Social Sciences Reviews, 7(5), 32-40. https://doi.org/10.18510/hssr.2019.754
33. Gandamayu, I. B. M., Antari, N. W. S., & Strisanti, I. A. S. (2022). The level of community compliance in implementing health protocols to prevent the spread of COVID-19. International Journal of Health & Medical Sciences, 5(2), 177-182. https://doi.org/10.21744/ijhms.v5n2.1897